ROTORDYNAMIC INSTABILITY FIELD PROBLEMS

J. C. Wachel
Southwest Research Institute
San Antonio, Texas   78284

SUMMARY

Vibration data obtained during several rotor instability investigations is presented to illustrate the effect of changes in system parameters on overall rotor stability. The data includes the effects of bearing and seal changes as well as those due to variations in speed and pressure ratio. Field problems indicate that the stability of rotors is often highly sensitive to fairly minor variations in bearing and seal parameters. Measured field data is valuable in normalizing analytical computer models so that effective solutions can be obtained.

INTRODUCTION

Rotor instability vibrations in compressors and turbines have occurred more frequently in recent years and have caused severe failures and costly downtime for several large projects. Rotor instabilities can occur in flexible shaft units which operate above their first critical speed. The whirling instability frequency is usually near one of the shaft critical speeds and can be caused by many factors, including hydrodynamic cross coupling of bearings and seals, internal friction, aerodynamic cross coupling, and torsional coupling. The whirling motion can be subsynchronous or supersynchronous, and may be forward or backward precession; however, in general most problems are subsynchronous and have forward whirl.

During the past few years, vibration data has been collected on several compressors that have experienced severe shaft instabilities. These compressors differed in manufacture, shaft diameter, weight, bearing span, critical speeds, and running speed. The spectral characteristics of shaft vibrations were observed as the compressors/turbines approached the onset of instability; i.e., before the machine experienced the high level vibrations normally associated with unbounded instabilities. On most units that have instability problems, a trace of vibration at some instability frequency normally exists at all times; however, it is not possible to verify the severity of the instability from vibration measurements at one operating condition. The threshold of instability can be fully defined only from testing over the full performance range of the machine, and even this approach is not always completely adequate. Some units have run satisfactorily for several years before serious instability trip-outs occurred. After one year of satisfactory operation, one compressor failed eight times in the next three years from instabilities. Because the stability margin on some units is so delicately balanced, its characteristics can be drastically changed whenever small changes are made in factors such as pressure ratio, flow, bearing clearance, oil temperature, unbalance, alignment, etc., or upsets in the process such as liquid slugs, surge transients, or electrical trip-outs.

It follows, therefore, that the threshold of stability can likewise be improved by small changes in these same parameters, but the exact improvement required to make an unstable system stable is sometimes difficult to predict.

The most sensitive elements which influence rotor stability include the following: (1) hydrodynamic cross coupling in fluid film bearings, seals, and labyrinths, (2) aerodynamic cross coupling forces, (3) hysteretic or internal friction damping, (4) pulsations, (5) pulsating torque and axial loads, (6) asymmetric shafting, (7) fluid trapped in rotor, (8) stick-slip rubs and chatter, (9) dry friction whip.

To properly calculate the stability margin of a rotor, the mathematical model must be able to simulate all possible destabilizing components. The logarithmic decrement evaluation of rotor system damping is useful for predicting rotor stability. Field experience shows that while this technique provides proper direction in designing for stability, uncertainty still exists in quantitatively predicting the onset of instability and defining the contribution of individual influencing parameters.

When instability vibrations occur in installed machinery, better estimates of the possible effects of system changes can be made if measured field data is available for normalization of the mathematical model. The normalization procedures compensate for unknown dimensional variations which affect bearing and seal properties and adjust for actual aerodynamic loading. This paper will present measured field data gathered over the past nine years on several machines which exhibited instabilities (ref. 1). The data analysis techniques presented were used to define rotor stability thresholds and the effects of modifications to seals, bearings, shafts, and process variations.

CASE 1. INSTABILITY OF A STEAM TURBINE

On startup of a steam turbine after a complete turn-around in which new pressure pad bearings were installed, the measured shaft vibrations indicated the turbine first critical speed was at 1800 rpm as shown in figure 1 which gives the amplitude and phase angle response versus speed. When the unit speed approached 4800 rpm, a subsynchronous instability at 1800 cpm suddenly appeared (fig. 2).

A stability analysis revealed that the calculated logarithmic decrement for this rotor with tight bearing clearances was only 0.04. Investigations were made into possible field modifications to improve the stability that could be implemented in a short time. Calculations showed that if the pressure pad bearing clearance was increased and the bearing length reduced, then the logarithmic decrement increased to 0.2 with the critical frequency remaining near 1800 cpm.

The bearings were then modified and installed. Vibration data with the new bearings is shown in figure 3. The turbine speed could be increased to 5100 rpm without any instability occurring and the unit has continued to operate without instabilities. This case illustrates that some instability problems can be solved by fairly simple modifications.

CASE 2. STEAM TURBINE INSTABILITY IN A METHANOL PLANT (ref. 2)

This case deals with a 13,000 hp, 10,600 rpm, three stage steam turbine. The rotor had pressure pad bearings at a bearing span of 236 cm (60 inches). The bearings were later changed to 5 shoe tilted pad bearings in an attempt to eliminate the half speed problems which occurred at maximum speed. Data taken during the turbine startup with the new bearings (fig. 4) revealed a vibration component at one-half speed when the speed reached 7200 rpm, thus showing that the change to tilted pad bearings was not sufficient to eliminate the half speed vibrations. During subse-

quent runs, two subharmonic criticals at 4500 and 7000 cpm were excited as well as the half speed component (fig. 5).

During another run a subsynchronous frequency occurred at approximately 0.3 times the running speed. Figure 6 shows that a large amplitude component occurred at 2500 cpm when the running speed was 9000 rpm. Both oil pumps were running during this test and one tripped out for a few seconds. The turbine running speed suddenly dropped 200 rpm. The instantaneous frequency analysis shown in the upper trace of figure 6 shows that this upset moved the subsynchronous component from 2500 to 4400 cpm. Frequency analyses made later showed that the subsynchronous vibration components were also different on the horizontal and vertical probes of the turbine (fig. 7). These two instability frequencies were near calculated damped instability frequencies.

Several modifications were implemented that reduced the magnitude of the instability. These included changing the seal design, increasing the bearing clearances, and strengthening the bearing housing. This case illustrates that changing to tilted pad bearings may improve the stability characteristics of a rotor but does not necessarily eliminate instabilities. With the tilted pad bearings for this rotor, however, only slight changes were required to control the instabilities.

CASE 3. INSTABILITY OF GAS REINJECTION COMPRESSOR (ref. 3)

This case deals with a much discussed reinjection compressor which experienced excessive nonsynchronous vibrations on startup. Field vibration data will be presented which shows the influence of oil ring seals, aerodynamic cross coupling, and speed on instability frequencies and amplitudes. These areas are of major concern to rotordynamists; however, very little experimental data is available in the open technical literature. The 22,000 horsepower, eight stage compressor with back-to-back impellers (fig. 8) was rated at 8500 rpm, had a design suction pressure of 24.1 MPa (3500 psi), and discharge pressure of 63.4 MPa (9200 psi). The calculated first critical speed of the rotor was 3800 cpm for a bearing span of 206 cm (81 inches). Floating oil seals were located a few inches inboard of the bearings. The compressor originally could not be brought to design speed and pressure without tripping out on high vibrations (fig. 9). The units were monitored by shaft vibration probes which automatically shut down the unit whenever the vibrations exceeded 64 μm (2.5 mils); however, due to the monitor's finite response time and suddenness of the instability trip-outs, vibration amplitudes equaling total bearing clearance were experienced.

The frequency of the nonsynchronous instability was 4400 cpm which was higher than the calculated rigid bearing critical speed of 4200 cpm. This can occur if the floating oil seals lock up and carry some load, thereby effectively reducing the bearing span. In the computer simulation of this shaft, an effective oil seal stiffness of 286,000 N/cm (500,000 lb/in) was required to calculate an instability frequency of 4400 cpm. Using this stiffness for the oil seals the calculated log decrement reduced to 0.08 compared to 0.3 calculated for the original rotor, neglecting the effect of the seals. Therefore, the calculations indicated that the seals significantly reduced the stability of the unit.

To improve the rotor instability, two circumferential grooves were cut into the sealing surface of the seals, the pressure balance of the rings was improved, and the coefficient of friction of the sliding surfaces was reduced. The compressor was still unstable, as can be seen in figure 10. A nonsynchronous instability occurred at 4700 cpm; however, instabilities above running speed at 9500 and 10,500 cpm were also excited. As the unit speed reduced, the instability component at 10,000 cpm

remained. The rotor was found to be sensitive to the rate of acceleration; therefore, by slowing down the startup procedure, it was possible to operate in the normal speed range.

To more fully define the stability limits, data was obtained throughout the entire performance map. For a constant speed of 7600 rpm, figure 11 shows how the aerodynamic loading affects the amplitude of the instability component at 5160 cpm (a forward precessional mode). As the suction pressure increased, the amplitude of the instability increased but remained within bounds until a limiting pressure was reached. The frequency of the instability component moved from 4400 to 5160 cpm as pressure was increased. To show the effect of speed on the instability the suction pressure was held constant at 10.3 MPa (1500 psi) and the speed increased. The instability amplitude increased almost linearly with speed (fig. 12).

After these tests were made, several seal designs were tested (fig. 13); however, there was little improvement in the overall rotor stability. The type of seal design greatly affected the frequency of the nonsynchronous instability and the threshold speed. One seal design studied had large radial clearances and only one land, less than 5 mm (0.2 inch) long. The test was primarily to study the effect on the instability frequency since the seal oil leakage was excessive. Shortening the seal length should reduce its load-carrying effect, thus reducing the instability frequency. However, test results showed that nonsynchronous instabilities occurred at frequencies above running speed (10,000 and 11,000 cpm) similar to the data presented in figure 10.

Another test using a different seal design also showed instabilities above running speed. These instability frequencies appeared to be a function of suction pressure as shown in figure 14. During this test the compressor speed was 7523 rpm and suction pressure 8.28 MPa (1200 psi). Figure 14 gives the frequency analysis showing 13 μm (0.5 mil) at running speed and 25 μm (1.0 mil) at 10,500 cpm and a trace at 4500 cpm. As the suction pressure was reduced, the higher frequency component lowered to 8900 cpm and then separated into two components, 8900 and 9300 cpm.

Some specifications require that the first critical speed be greater than 0.6 times the running speed to help prevent instabilities. Figure 15 shows that an instability component at 0.8 times running speed occurred when the running speed was 4000 rpm or slightly above the first critical speed. In this data, the instability occurred when the ratio of running speed to first critical was 1.25, showing that a ratio of running speed to first critical of less than 2:1 does not necessarily ensure that a rotor will be stable. The majority of the instability trip-outs were at speeds where the ratio of running speed to first critical speed was less than 2:1.

The data presented shows that the stability frequency characteristics were dramatically changed by changing only the oil seals; however, no change in seal design made this system stable. This indicates that the seals were not the predominant destabilizing factor.

Major efforts were then expended to reduce other destabilizing factors. These changes included aerodynamic changes to the impellers and diffusers, seal modifications, shortening the bearing span, and changing the bearings to 5 shoe, nonpreloaded tilted pad bearings. Log decrement calculations indicated that these changes represented a significant improvement in the rotor stability.

Even after these modifications were installed, instabilities still occurred. On startup, an instability component (5200 cpm) was present with a fluctuating ampli-

tude. The instability frequency then shifted up to 5800 cpm, and the amplitude jumped to greater than 152 μm (6 mils) in approximately one second. The instability component was particularly sensitive to pressure ratio across the machine, which confirmed that the aerodynamic destabilizing effects were of major importance and overshadowed other improvements that were made.

The stability of the unit was markedly improved when a damper bearing was installed in series with the inboard bearing. Squeeze film damper bearings employ an oil film in the space between the outside of the bearing and the case, to which oil is continuously supplied. Stiffness of the damper bearing is usually supplied by a mechanical support such as a squirrel cage cylinder with ribs, welded rod support, corrugated metal ring, or o-rings. Figure 16 gives the frequency analysis of the shaft vibrations and two probes monitoring the damper bearing for 8450 rpm with a suction pressure of 23.1 MPa (3350 psi) and a discharge pressure of 56.9 MPa (8250 psi). Instability frequencies were still present, but the added damping from the damper bearing prevented the amplitudes from becoming unbounded. The improvement in the stability characteristics of this rotor illustrates the potential of damper bearings in high pressure applications.

At the time of this study, the mathematical techniques for predicting instabilities were not as developed as today's procedures and the application of a damper to an industrial compressor involved some tuning to obtain the optimum stiffness and damping for an individual rotor. This can be amply illustrated by the fact that a damper bearing installed in a second identical unit was not successful in eliminating instability trip-outs (fig. 17). After some tuning of the damper bearing, the stability was significantly improved.

In the process of evaluating the performance of the damper bearing, the oil temperature was varied to determine if it had a significant effect. At an oil temperature of 51° C (124° F), the frequency analysis of shaft vibrations showed instability components at 2800 and 4800 cpm along with the running speed component. Some surprising results were noted as the temperature was lowered. At a temperature of approximately 48.9° C (120° F), the 6 μm (0.25 mil) component at 2800 cpm disappeared (fig. 18). Again this points out that very small changes can be significant to the stability of a rotor.

This case history illustrates that many factors influence the onset, frequency and amplitude of instability vibrations, and that sophisticated mathematical models are required to simulate the instability phenomena measured in these machines.

This instability problem was controlled primarily by increasing the shaft diameter to raise the first critical speed, thus significantly increasing the ability of the shaft to withstand the large aerodynamic loading effects.

Aerodynamic loading effects are the most predominant destabilizing components in many high pressure systems. In the design stage the designer needs to estimate the level of equivalent aerodynamic loading so that the rotor will have an adequate stability margin. The author has consulted on several instability problems and has developed an empirical formula for estimating the level of aerodynamic loading (ref. 4).

$$K_{xy} = \frac{B(hp)(Mol\ Wt)}{Dhf} \frac{\rho_D}{\rho_S}$$

5

K_{xy} = aerodynamic loading, N/m (lb/in)

B = cross coupling constant, 16 (105)

hp = power, kW (hp)

Mol Wt = molecular weight

D = impeller diameter, m (in)

h = restrictive dimension in flow path, m (in)

f = speed, Hz

ρ_D = density of fluid at discharge conditions, kg/m^3 (lb/cu ft)

ρ_S = density of fluid at suction conditions, kg/m^3 (lb/cu ft)

When this formula was applied to several rotors that had instabilities, it appeared to give overall levels of aerodynamic loading near that required to cause the logarithmic decrement to be negative. This equation is presented so that it may be further evaluated.

CASE 4. INSTABILITY OF ATOMIZER SHAFT

An atomizer was driven by a 250 hp, 3600 rpm, electric motor through a variable speed transmission over a speed range between 10,000 and 13,500 rpm. A slurry was pumped by positive displacement pumps to the atomizer which was mounted on top of a large cone-shaped tank. The slurry was then sprayed into the tank and was instantly dried by hot air which was blown directly at the atomizer wheel. The heated air was forced through the heater and into the tank by a forced draft fan. The dried powder was then drawn out of the tank by an induced draft fan into a bag house where the powder was collected. Upon startup, high vibrations were experienced on the atomizer shaft, resulting in several shaft failures near a carbon bushing. A field investigation was made to determine the causes of the high vibration and failures and to develop a solution.

During the tests the atomizer shaft vibrations were measured with a proximity probe mounted inside the atomizer housing approximately 15.2 cm (6 inches) above the carbon bushing (fig. 19). Torsional vibrations were measured with a CEC torsiograph mounted on a special stub shaft attached to the motor shaft. Pulsations in the liquid feed line and the tank near the atomizer wheel were measured with pressure transducers. Vibrations on the atomizer, gearbox, and motor were measured with accelerometers.

Several tests were made, including running the unit without condensate or slurry, running with water alone, running with fans on but atomizer off, running with heater only at a low feed rate, and shock excitation runs to determine natural frequencies.

When the shaft was run dry, two instability frequencies at 12 and 26 Hz were indicated in the real time spectral analysis of the proximity probe measurements of the carbon. When the unit was run with condensate water, the amplitudes at the instabilities increased (fig. 20). The vibrations at the forward whirl mode occurred first and built up until the shaft touched the carbon bushing which caused a backward whirl mode to be excited at 12 Hz. Measured pulsations at the slurry input showed pulsations at 26 Hz which could excite the forward mode at 26 Hz. The sensitivity of

6

the instability modes can be seen in figure 21. When the vibrations were measured over the range of flow rates, the vibrations became severe as shown in figure 22.

Based upon the analysis of the data, it was determined that the excitation for the instability was the pulsative fluid flow. The atomizer was designed for a feed rate of 50 cubic meters per hour; however, the maximum flow rate was only 19 cubic meters per hour. The atomizer was creating a vacuum in the feed header line even at full flow rates. This caused the liquid to enter the atomizer in slugs rather than a smooth flow. The liquid slugs entering the atomizer wheel acted as destabilizing forces which caused the forward whirl.

Several modifications were implemented to improve the inlet flow characteristics. The distributor flow area was reduced approximately 70% by an orifice restrictor and the inlet feed tube diameters were reduced and connected together through a "Y" connection.

These modifications on the inlet flow lines and the new distributor improved the inlet flow characteristics and reduced the instability vibration amplitudes; however, the shaft continued to rub against the carbon bushing under all flow conditions. Plugs were then installed in 12 of the 24 discharge holes in the atomizer wheel to further restrict the flow rate.

After these modifications were installed, the vibrations were low (fig. 23) and the shaft no longer rubbed against the carbon bushing. The atomizers have run successfully without failures since 1977.

This case history illustrates that if the excitation source for an instability can be identified and reduced, the instability can be controlled without shaft modifications.

REFERENCES

1. Wachel, J. C., Case Histories of Rotordynamic Installations in the Field, Short
       Course on Rotordynamics of Turbomachinery, Texas A&M University, College
       Station, Texas, May 18-20, 1981.

2. Wachel, J. C., Turbine and Compressor Vibration, Ammonia Plant Safety, vol. 15,
       1973, American Institute of Mechanical Engineers, pp. 69-76.

3. Wachel, J. C., Nonsynchronous Instability of Centrifugal Compressors, ASME Paper
       75-Pet-22.

4. Wachel, J. C. and W. W. von Nimitz, Ensuring the Reliability of Offshore Gas
       Compressor Systems, Society of Petroleum Engineers of AIME, Journal of
       Petroleum Technology, Nov. 1981, pp. 2252-2260.
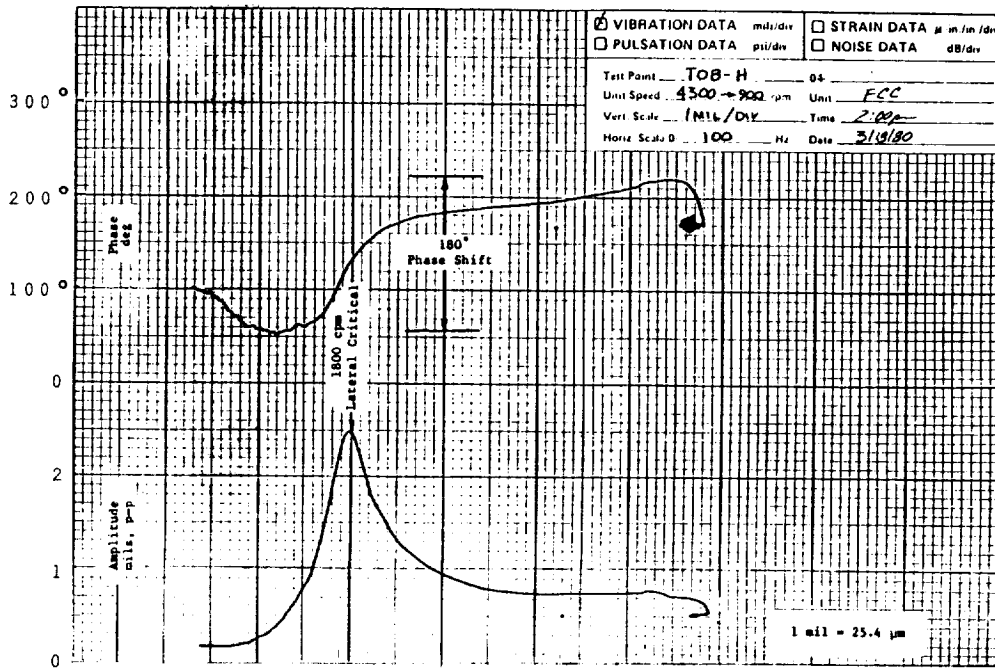
Figure 1. - Vibration and phase angle measured during shutdown.
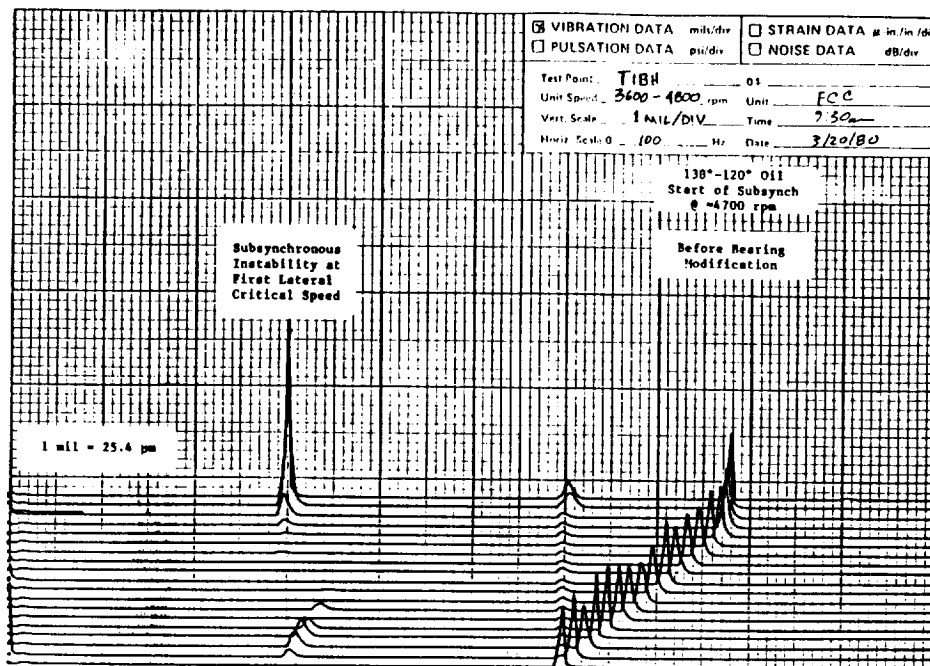
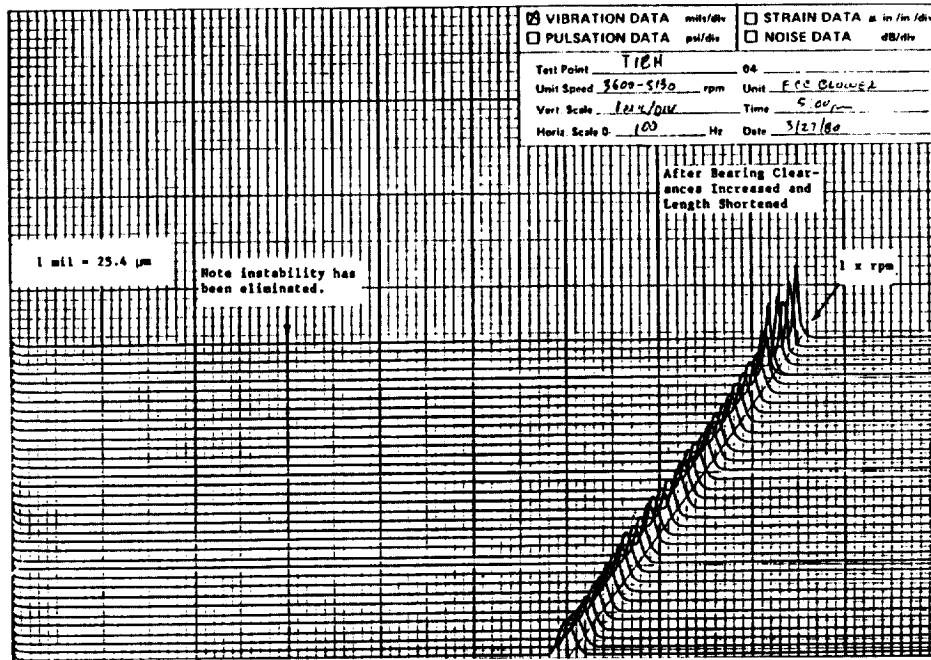Figure 2. - Subsynchronous instability excited on turbine.

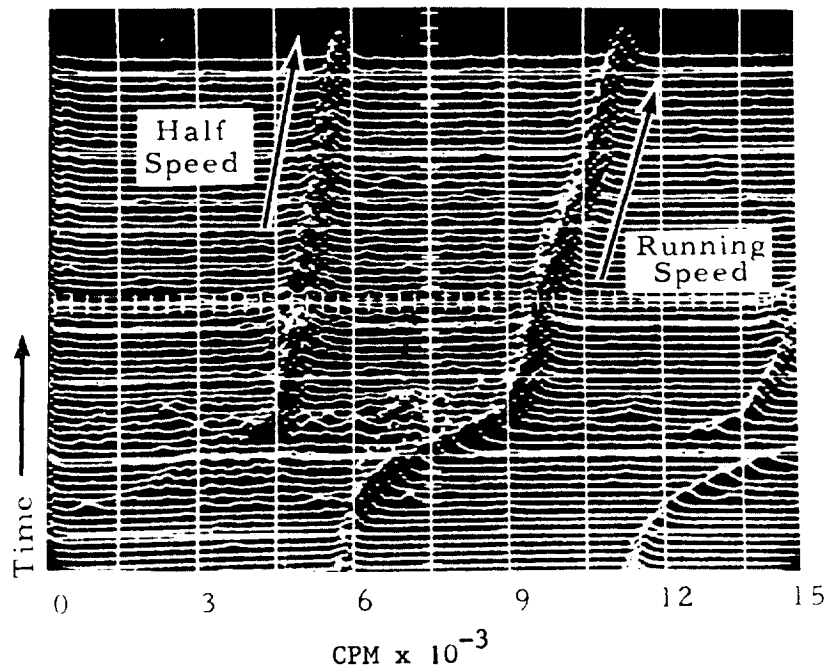Figure 3. - Elimination of instability by bearing modification.

Figure 4. - Spectral time history of half speed vibrations on turbine with tilted pad bearings.
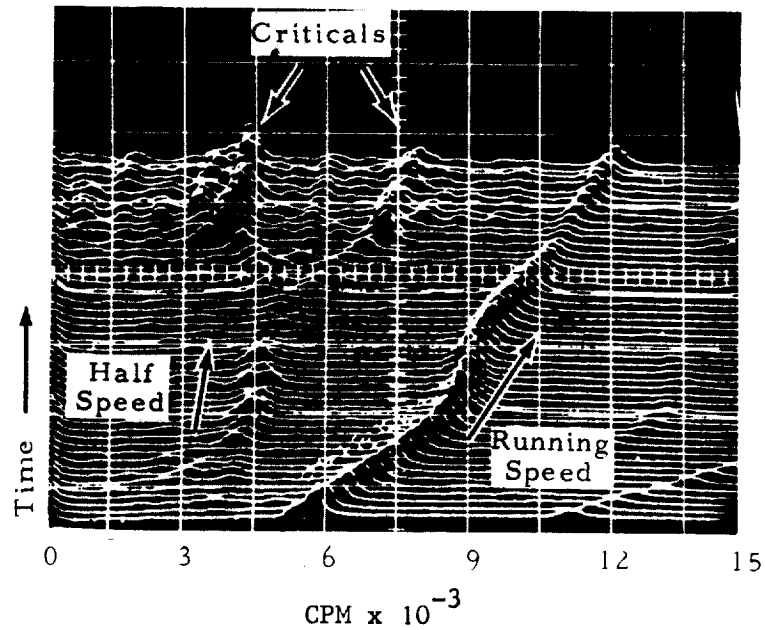
9

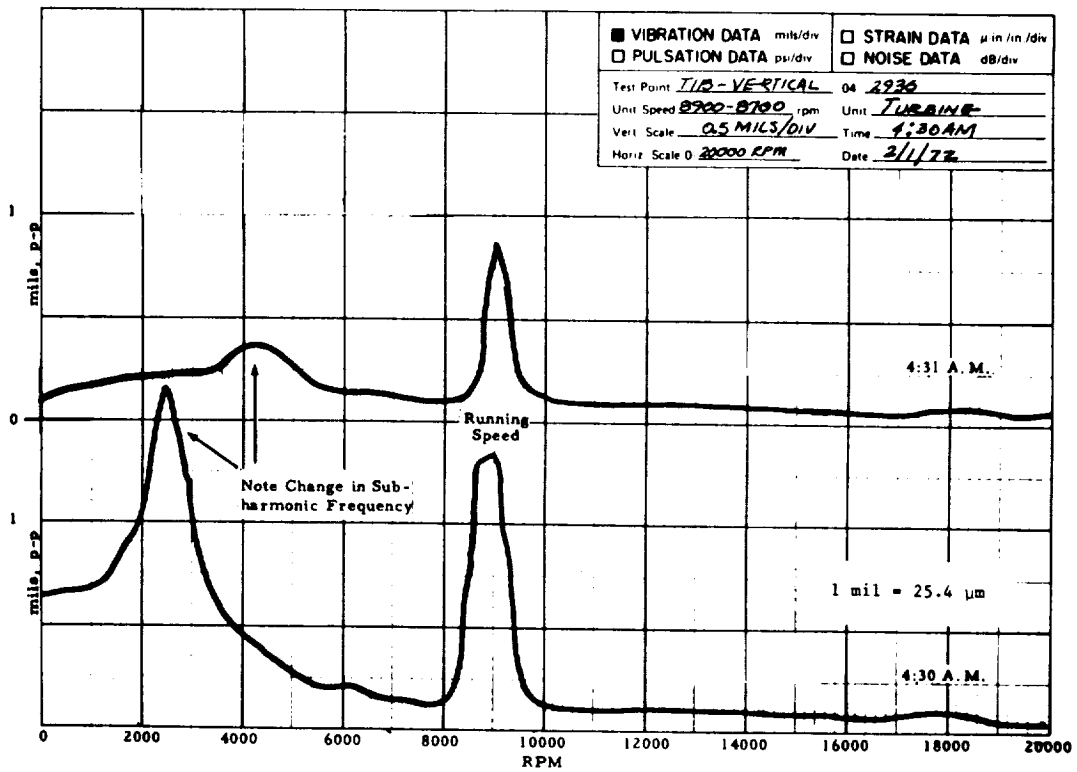**Figure 5. - Spectral time history of turbine showing subharmonic vibrations in normal speed range.**
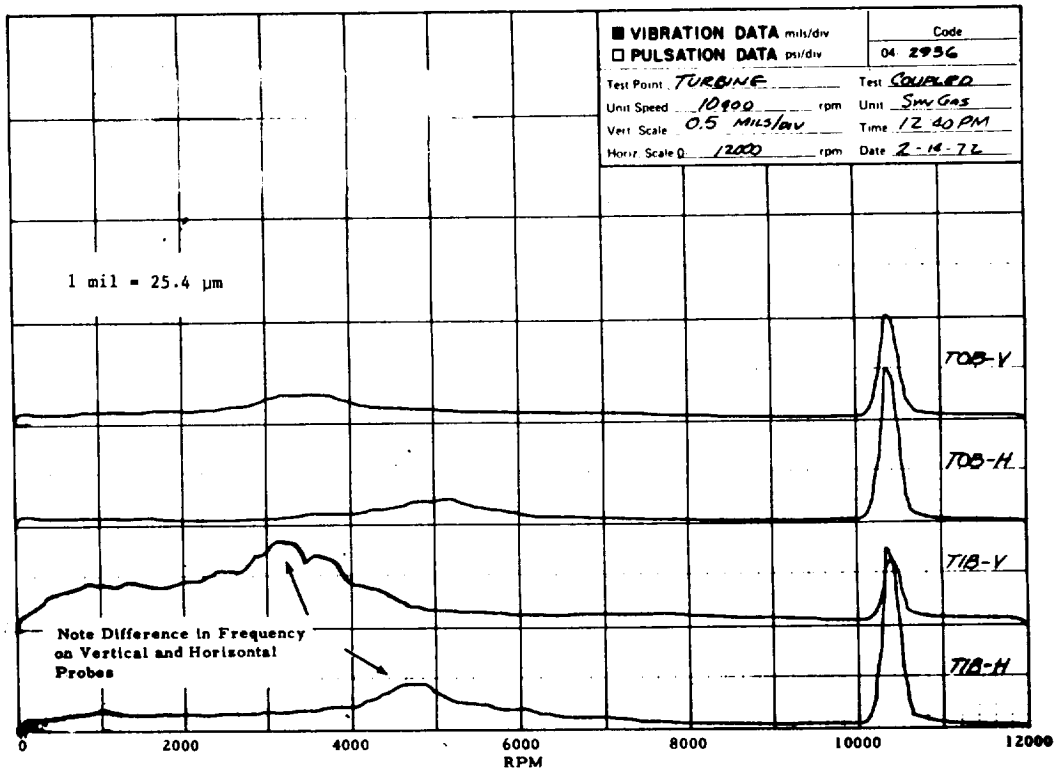

Figure 6. - Subharmonic vibrations of turbine.

Figure 7. - Subharmonic turbine vibrations measured at 10400 RPM.
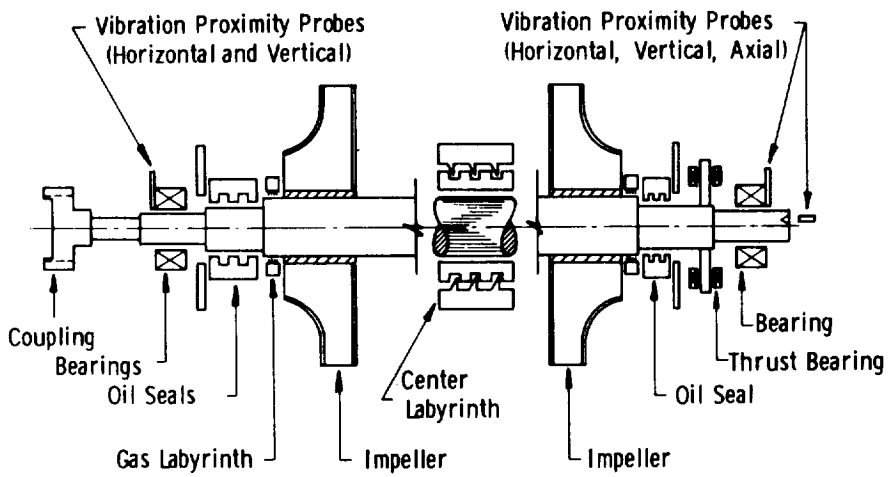
Figure 8. - Typical high pressure compressor design.

11
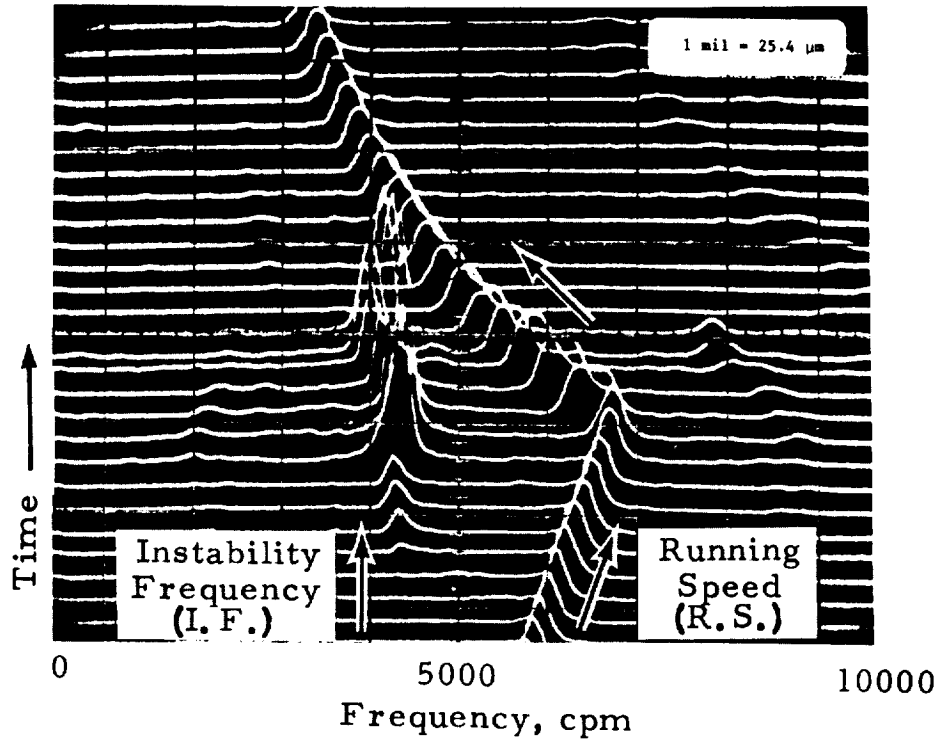
Figure 9. - Tripout of compressor as speed is increased.
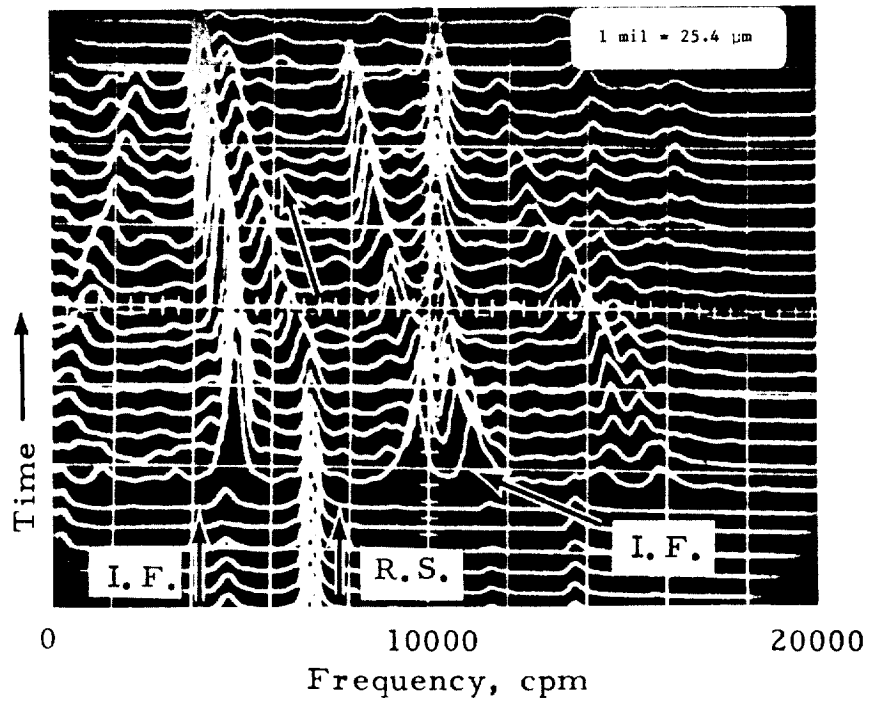
Figure 10. - Compressor instability with improved seal design.
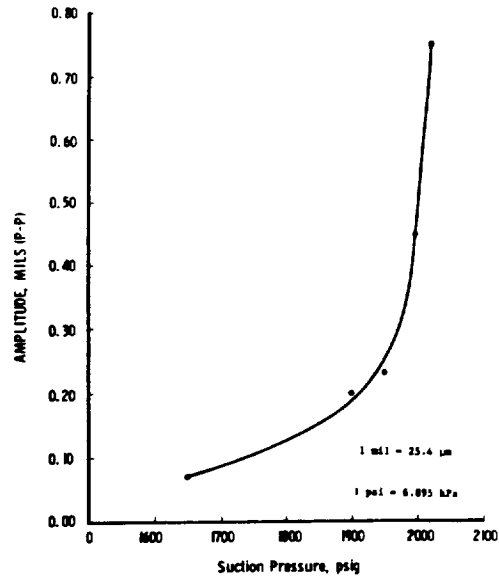
Figure 11. - Instability amplitude versus suction pressure.
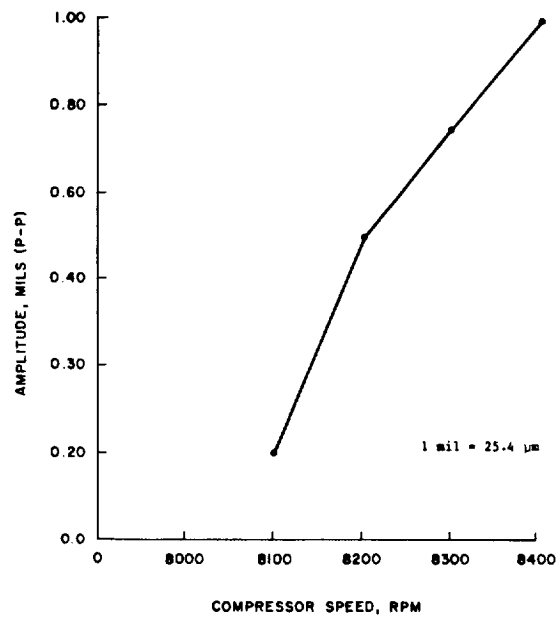
Figure 12. - Instability amplitude versus compressor speed.

Mod. 1
(1) Teflon O-rings
(2) Teflon coating on sealing surfaces
(3) Two circumferential grooves
(4) Machine shoulder to balance pressure

Mod. 2
(1) Original seals
(2) No O-rings
(3) Teflon coating on sealing surfaces
(4) Three oil dams at 120° intervals

Mod. 3
Basic Mod. 1 seal with two downstream lands removed

Mod. 4
(1) Original seals
(2) Three per seal assembly
(3) Upstream edge beveled
(4) Teflon O-rings

Mod. 5
(1) No O-rings
(2) Circumferential groove
(3) Reduced unbalanced pressures using peripheral lugs
(4) Teflon coating of sealing surfaces

Mod. 6
Identical to Mod. 5 except that only two seals were used per end

Mod. 7
Basic Mod. 1 seal with axial grooves replacing circumferential grooves

Figure 13. - Oil seal designs tested.
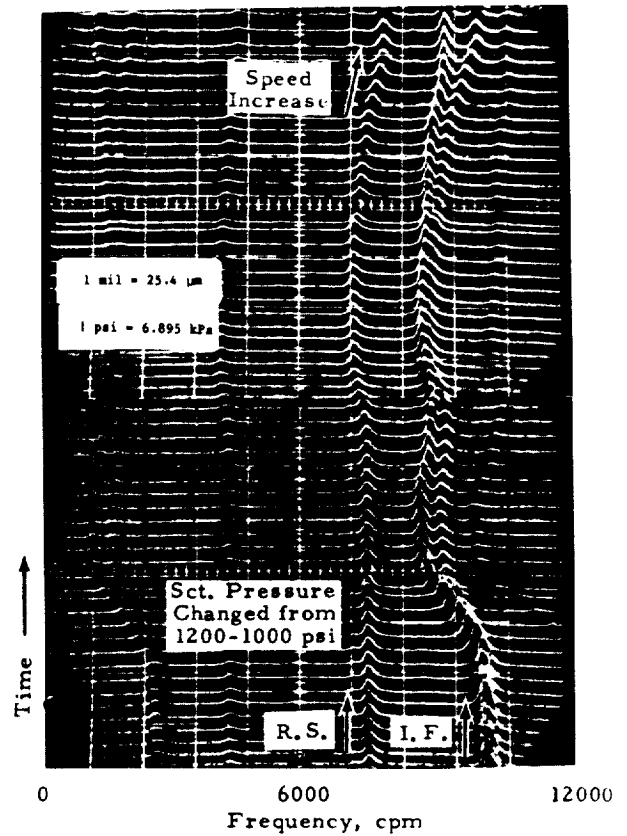
Figure 14. - Variation of instability frequency with suction pressure.

14
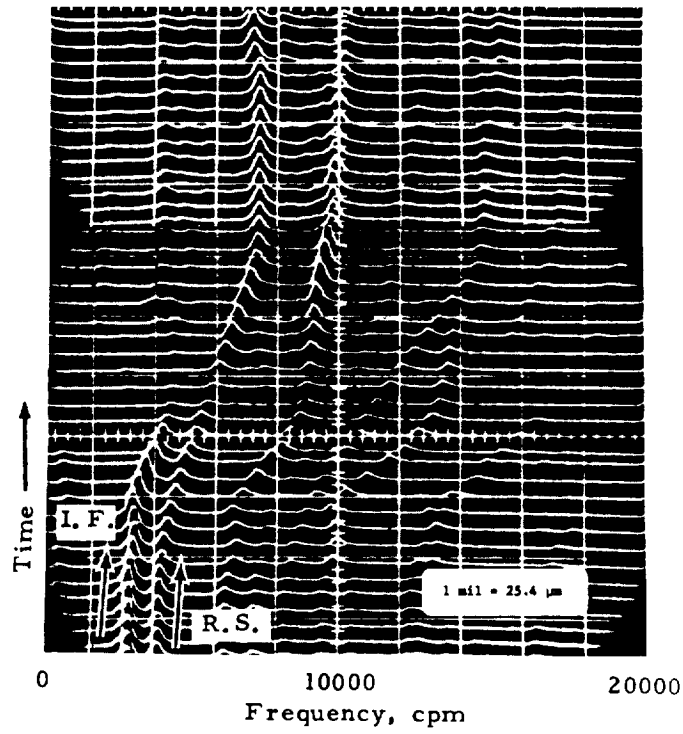
Figure 15. - Instability excited as compressor goes through first critical.
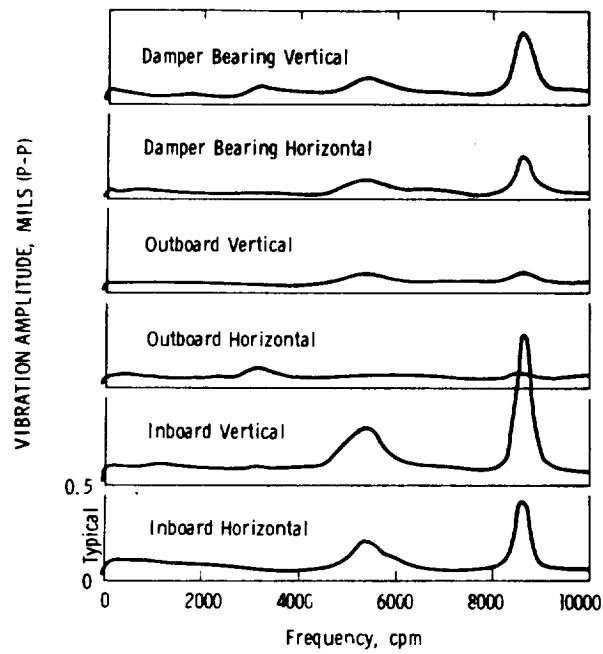
Figure 16. - Frequency analysis of shaft and damper bearing vibration with discharge pressure of 8250 PSI (56.9 MPa).
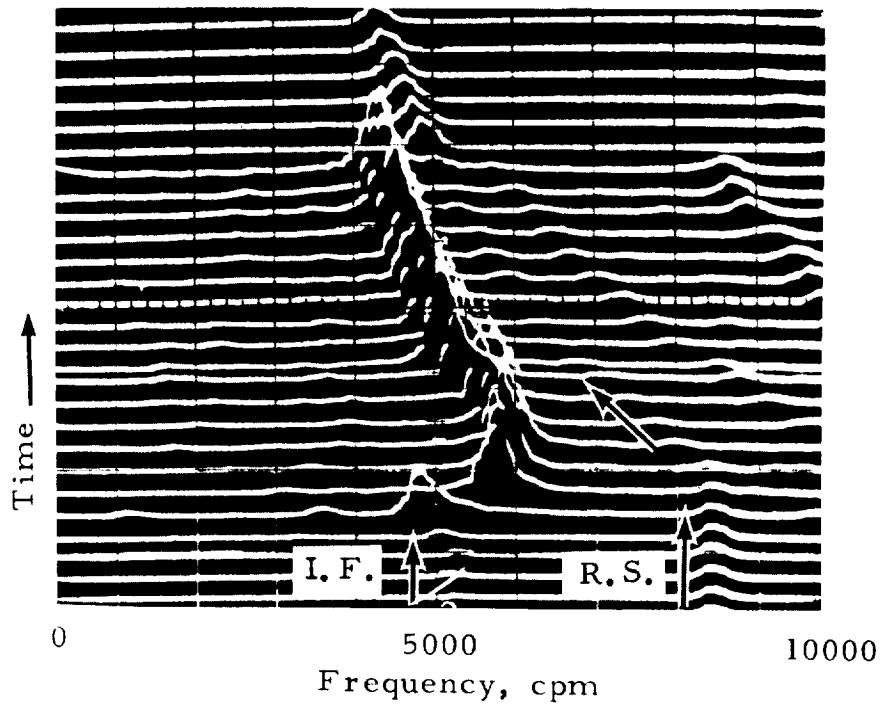
15

Figure 17. - Instability tripout of rotor with damper bearing installed.
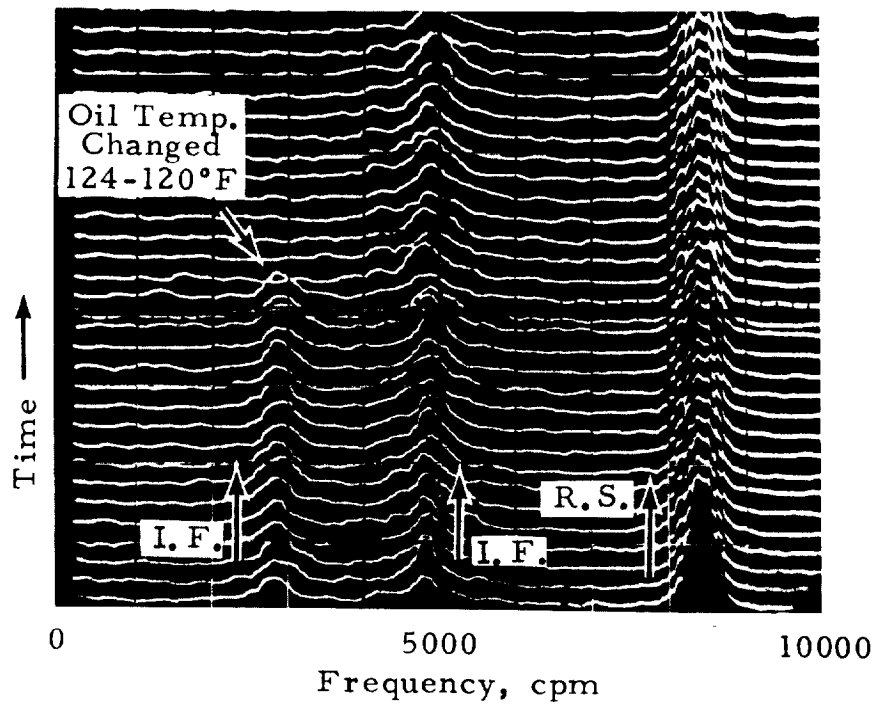

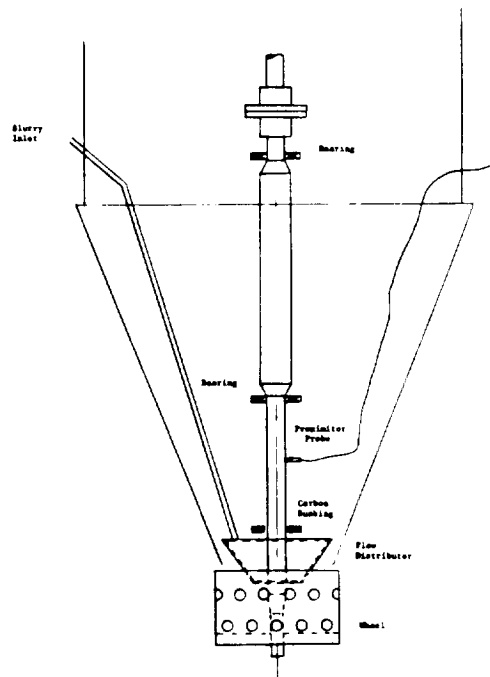Figure 18. - Elimination of instability component as oil temperature reduced.

16

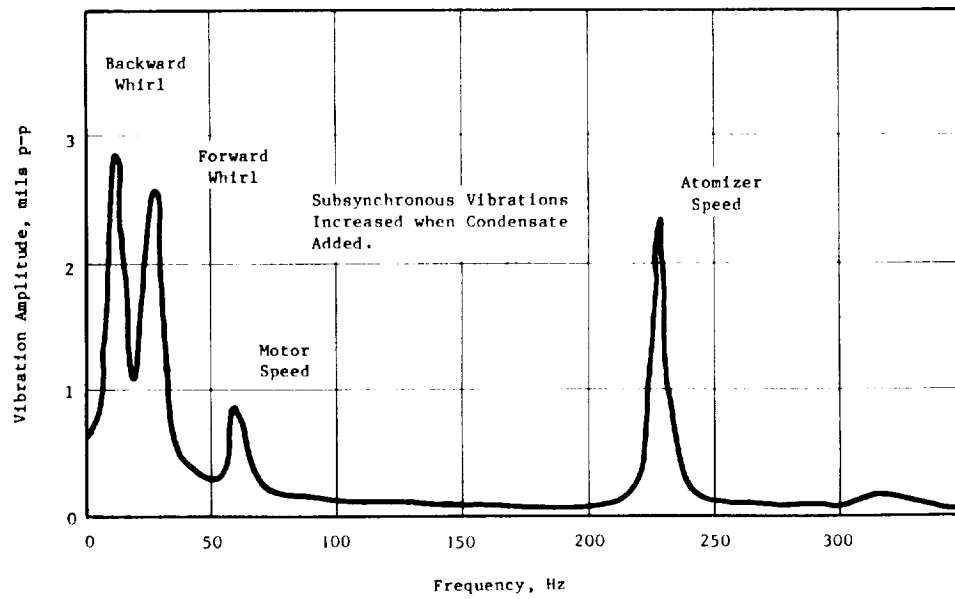Figure 19. - Cutaway view of atomizer.

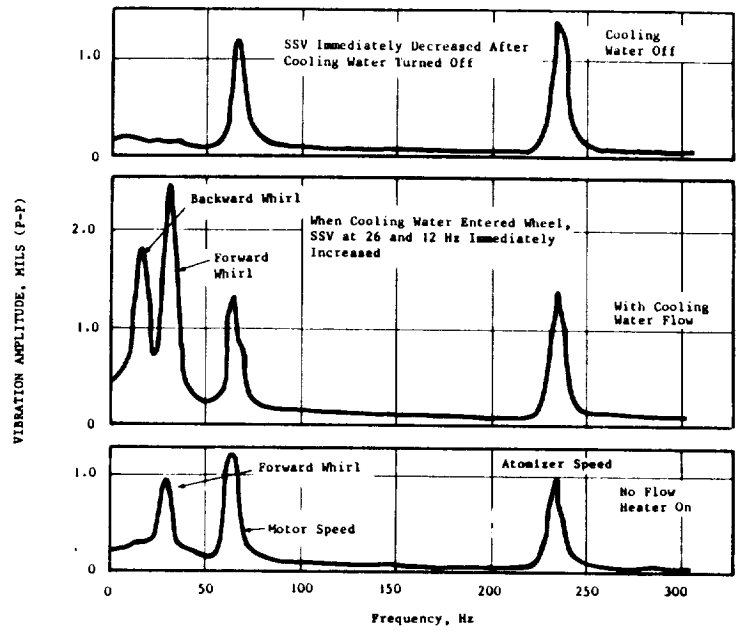Figure 20. - Instabilities excited on atomizer.

17

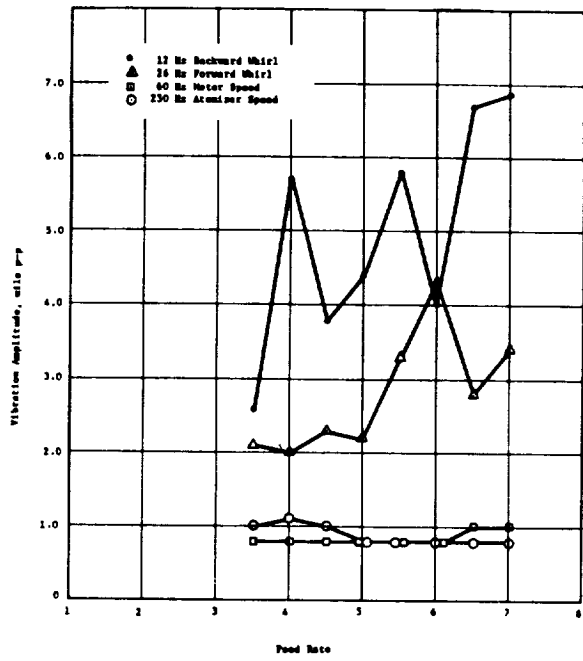Figure 21. - Effect of fluid flow on instabilities.
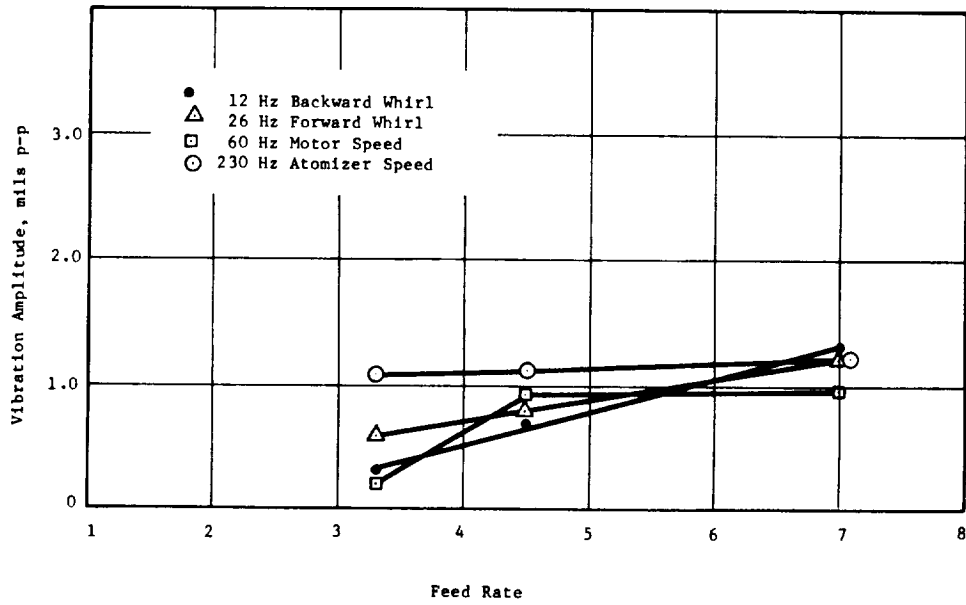
Figure 22. - Plot of atomizer shaft vibrations versus feed rate.

18

Figure 23. - Atomizer shaft vibrations after modifications.